JACS
JOURNAL OF THE AMERICAN CHEMICAL SOCIETY
pubs.acs.org/JACS
Article

Design Principles for Using Amphiphilic Polymers To Create Microporous Water

Christopher DelRe, Hyukhun Hong, Malia B. Wenny, Daniel P. Erdosy, Joy Cho, Byeongdu Lee, and Jarad A. Mason*

Cite This: J. Am. Chem. Soc. 2023, 145, 19982−19988
Read Online

ABSTRACT: Aqueous dispersions of microporous nanocrystals with dry, gas-accessible pores—referred to as "microporous water"—enable high densities of gas molecules to be transported through water. For many applications of microporous water, generalizable strategies are required to functionalize the external surface of microporous particles to control their dispersibility, stability, and interactions with other solution-phase components—including catalysts, proteins, and cells—while retaining as much of their internal pore volume as possible. Here, we establish design principles for the noncovalent surface functionalization of hydrophobic metal−organic frameworks with amphiphilic polymers that render the particles dispersible in water and enhance their hydrolytic stability. Specifically, we show that block co-polymers with persistence lengths that exceed the micropore aperture size of zeolitic imidazolate frameworks (ZIFs) can dramatically enhance ZIF particle dispersibility and stability while preserving porosity and >80% of the theoretical O_2 carrying capacity. Moreover, enhancements in hydrolytic stability are greatest when the polymer can form strong bonds to exposed metal sites on the external particle surface. More broadly, our insights provide guidelines for controlling the interface between polymers and metal−organic framework particles in aqueous environments to augment the properties of microporous water.

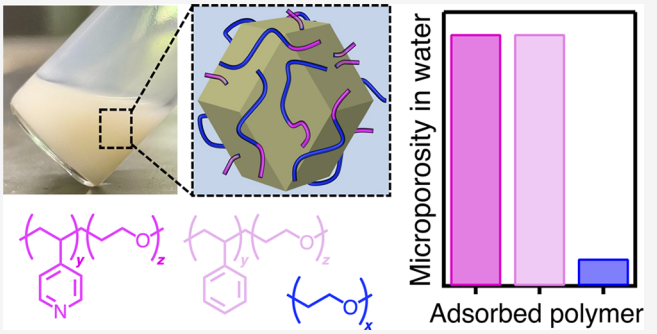

INTRODUCTION

The low solubility of gases in water is a critical challenge for many energy and biomedical technologies that require high concentrations of gas molecules to be rapidly transported through an aqueous environment.[1−5] Owing to their high internal surface areas,[6,7] microporous materials—such as zeolites and metal−organic frameworks—can be used to dramatically enhance the gas density contained within an aqueous fluid, provided colloidally stable aqueous dispersions can be formed in which the micropores remain dry and accessible to gas molecules.[8] Such dispersions—termed "microporous water"—are possible when microporous particles are constructed with external surfaces that are sufficiently hydrophilic to promote dispersibility in water and internal surfaces that are sufficiently hydrophobic to make it thermodynamically unfavorable for liquid water to intrude into the pores.

The internal surface chemistry of a microporous particle is dictated by the composition and structure of the material, while the external surface can be modified through both covalent and noncovalent functionalization strategies.[9−11] This modularity creates myriad possibilities for microporous water with a wide range of properties and functionalities. In principle, the internal and external surfaces of microporous particles can be independently manipulated to design aqueous fluids with gas carrying capacities, gas selectivities, gas transport kinetics, colloidal stabilities, and biocompatibilities that are tailored to the requirements of a particular application. External surface functionalization is particularly important for enhancing colloidal stability and biocompatibility,[10,12] but can be challenging to carry out in a manner that preserves complete access of guest molecules to the internal pores of the framework.[13]

The noncovalent association of polymers offers a generalizable and highly tunable approach to functionalize the surface of colloidal nanoparticles. Polymers readily adsorb to the surface of many nanoparticles—often independent of their surface chemistry—due to surface tension reduction and favorable enthalpic and/or entropic interactions.[14−17] The adsorbed polymer layer can then improve the colloidal dispersibility of the nanoparticles through repulsive electro-

Received: June 22, 2023
Published: September 1, 2023

https://doi.org/10.1021/jacs.3c06627
J. Am. Chem. Soc. 2023, 145, 19982−19988

static or steric interactions.[18] In addition, polymers such as polyethylene glycol (PEG) can improve biocompatibility by inhibiting protein adsorption, immune responses, and cellular internalization.[19] Beyond biocompatibility and colloidal dispersibility, the noncovalent complexation of polymers offers a potential pathway to manipulate the stability—or dissolution rate—of water-sensitive metal−organic frameworks through control over the framework−water interface.[20−22]

Though composite materials composed of polymers and metal−organic frameworks or zeolites have received a lot of attention—particularly in the context of mixed-matrix membranes for gas separations[23,24]—much remains to be understood about interactions between polymers and crystalline microporous nanoparticles in aqueous solutions.[13,25,26] In order to be useful for microporous water, polymer adsorption must be confined to the external surface of the microporous particles and must not lead to blockage of pore entrances or filling of pore channels.

Herein, we report design principles for using polymers to disperse hydrophobic metal−organic frameworks in water while preserving their internal porosity and enhancing their stability. When appropriately designed, polymer coatings comprising amphiphilic block copolymers allow for the formation of colloidally stable and permanently porous dispersions of hydrophobic zeolitic imidazolate frameworks (ZIFs) that would otherwise aggregate and settle out of an aqueous solution. Moreover, dramatic enhancements in resistance to hydrolytic degradation are observed when the polymers contain functional groups that can form coordination bonds with exposed metal centers on the external surface of the frameworks. Through a systematic investigation of how chain rigidity, polymer concentration, and particle size affect the surface adsorption and micropore intrusion behavior of amphiphilic polymers, we provide insights into interactions between polymers and metal−organic frameworks in aqueous environments that offer new opportunities for designing microporous water and—more broadly—for synthesizing composite materials that leverage the unique properties of both polymers and microporous materials.

RESULTS AND DISCUSSION

The polymer PEG is routinely used to functionalize nanoparticles because its inherent amphiphilicity allows it to adsorb to most surfaces and facilitate particle dispersibility in a wide range of solvents, including water.[27] However, PEG contains a narrow and flexible backbone with a persistence length—the length below which the polymer behaves as a rigid rod—of only ∼3.5−4 Å.[28] As a result, PEG chains can uncoil and thread into the pores of many metal−organic frameworks in polymer melts,[29] organic solvents,[30] and water,[8] which substantially reduces—or entirely eliminates—their gas uptake capacity.

We hypothesized that attaching a bulky aromatic polymer block to PEG could prevent polymer intrusion and provide a generalizable strategy for dispersing hydrophobic metal−organic frameworks in water while preserving their internal porosity (Figure 1). Specifically, we selected blocks of poly(styrene) (PS) and poly(4-vinyl pyridine) (P4VP), whose bulky side groups and persistence lengths of at least ∼8 Å in polar solvents[31] would likely make it difficult for polymer chains to diffuse through narrow micropore apertures. Further, the pyridine side groups in P4VP could, in principle, coordinate to exposed metal sites on the external surface of

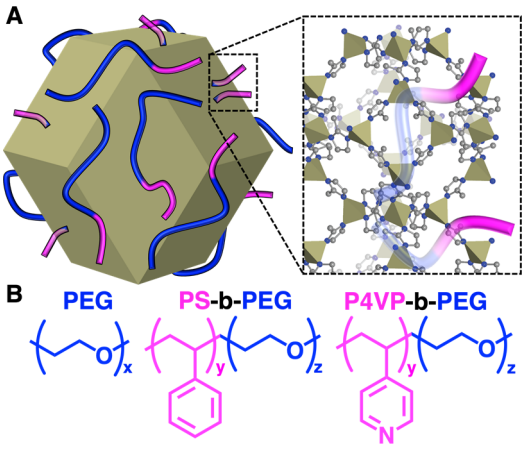

Figure 1. (A) Schematic illustration of polymer chains adsorbing to a ZIF particle and infiltrating into the framework micropores. (B) Structures of the three polymers used in this study.

metal−organic framework particles,[25,32] which would increase the polymer adsorption strength and provide insight into the relative roles of thermodynamics and sterics in preventing polymer infiltration. In addition, since many hydrophobic metal−organic frameworks are inherently unstable in water due to labile metal−ligand coordination bonds,[33] we anticipated that more strongly associated amphiphilic polymers might provide a mechanism to enhance hydrolytic stability by reducing the accessibility of water to the external surface of the particles.[34,35]

We chose $Zn(mIm)_2$ (ZIF-8; mIm = 2-methylimidazolate)[36] and $Co(mIm)_2$ (ZIF-67)[37] as model hydrophobic frameworks to test our functionalization strategy, since both frameworks contain hydrophobic pores that resist water intrusion under ambient conditions,[38,39] are not inherently dispersible in water,[8] can be synthesized as nanocrystals over a wide particle size range,[40] and degrade in aqueous solutions (especially at low concentrations).[41] For this study, we selected three different PEG molecular weights (1, 10, and 35 kDa) and diblock copolymers with comparable PEG lengths (3.5-b-10 and 4.5-b-34 kDa for P4VP-b-PEG, and 3.2-b-11 and 3.4-b-34 kDa for PS-b-PEG).

Dispersibility of Polymer-Functionalized ZIF Particles. All three amphiphilic polymers we tested—PEG, PS-b-PEG, and P4VP-b-PEG—dispersed ZIF-8 and ZIF-67 nanocrystals over a wide particle size range (45 to 900 nm in diameter, Figure S1) in water above a threshold polymer-to-ZIF mass ratio. ZIF nanocrystals smaller than 100 nm required a polymer:ZIF ratio of at least 2:1 to be dispersible in water (Figure 2A,C), while ZIF nanocrystals larger than 200 nm required ratios of at least 1:1 (Figure 2B,D). This difference is likely due to the increased external surface area-to-volume ratio of smaller nanocrystals, which would require more polymer chains to cover their external surfaces at a fixed mass concentration. Below the threshold polymer:ZIF ratios, or in the absence of polymer, ZIF nanocrystals rapidly aggregate and settle out of water. We note that the molecular weight of the polymer did not have a strong effect on ZIF dispersibility, and we did not observe any substantial differences between the dispersibility of ZIF-8 and ZIF-67 nanocrystals of similar sizes.

Porosity in Aqueous Dispersions of Polymer-Functionalized ZIF Particles. With all polymer-functionalized ZIF nanocrystals exhibiting high colloidal stability, we next

https://doi.org/10.1021/jacs.3c06627
J. Am. Chem. Soc. 2023, 145, 19982−19988

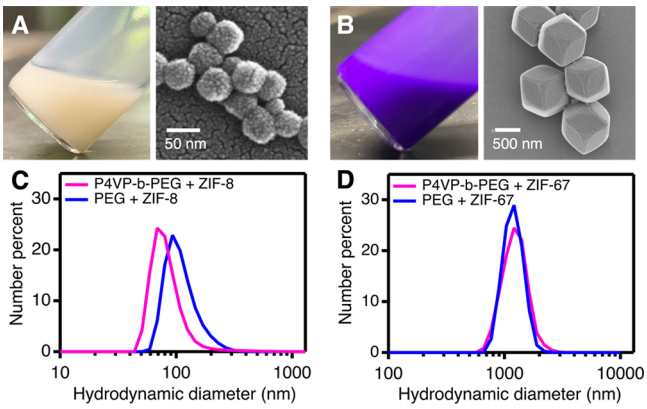

Figure 2. (A) Left: image of a P4VP-b-PEG/ZIF-8_{45nm} dispersion in water. Right: Representative scanning electron microscope (SEM) image of as-synthesized ZIF-8_{45nm} particles (the smaller particles that coat ZIF-8 and the substrate result from sputter coating with Pt/Pd to increase contrast during imaging) (B) Left: image of P4VP-b-PEG/ZIF-$67_{910\ nm}$ dispersions in water. Right: Representative SEM image of as-synthesized ZIF-67_{910nm} particles. (C) Particle size distributions determined by dynamic light scattering (DLS) for ZIF-8_{45nm} dispersed in water by P4VP-b-PEG (pink) or PEG (blue). (D) Particle size distributions determined by DLS for of ZIF-67_{910nm} dispersed in water by P4VP-b-PEG (pink) or PEG (blue).

investigated the impact of the PS and P4VP blocks on polymer infiltration behavior by evaluating the gas-accessible microporosity present in each aqueous dispersion. Specifically, we used an O_2 electrode to measure the amount of O_2 released when air-equilibrated dispersions were injected into deoxygenated water (Figure 3A, Table S1). Since the O_2 carrying capacity of each dispersion should be correlated with the accessible internal surface area of the ZIF particles, these O_2 release measurements serve as a direct and convenient probe of the degree of polymer infiltration in solution. We note that this approach is different from many other techniques to quantify polymer infiltration in microporous materials—such as surface area analysis,[42] NMR,[29] or X-ray diffraction[43]—that typically require solid samples.

Consistent with previous results,[8] pure PEG over a range of molecular weights (1, 10, and 35 kDa) resulted in a greater than 85% reduction of the O_2 carrying capacity of aqueous dispersions of ZIF-67 and ZIF-8 particles at a 1:1 polymer-to-ZIF mass ratio (Figure 3B). This result confirms that PEG chains—regardless of their length—are sufficiently flexible and narrow to uncoil and diffuse through the pore apertures of ZIF-8 and ZIF-67 and that PEG intrusion is thermodynamically favorable in water. We note that while PEG is water soluble, it is an amphiphilic polymer with high solubility in some nonpolar solvents as well. In contrast to pure PEG, dispersions of $PS_{3.2kDa}$-b-PEG_{11kDa} and $P4VP_{3.5kDa}$-b-PEG_{10kDa} copolymers at the same 1:1 polymer:ZIF ratios maintained over 75% of their O_2 carrying capacity (Figure 3B). In contrast, solid-state N_2 adsorption isotherms of dried samples at 77 K indicated no gas-accessible porosity after polymer functionalization, which could be attributed to changes in the arrangement of polymers at the particle surface or the degree of polymer intrusion upon drying, as well as the polymers having far less mobility and flexibility at cryogenic temperatures (Figure S2A). Moreover, this highlights that traditional methods for characterizing microporous materials do not necessarily reflect the porosity that will be present within an aqueous dispersion.

To evaluate whether the higher gas capacity—and accessible pore volume—of the copolymer-functionalized ZIF nanocrystals compared to PEG-functionalized nanocrystals was due to a difference in the strength of polymer binding or the polymer intrusion behavior, we adjusted the polymer concentration in solution until dispersions of PEG/ZIF-67 and P4VP-b-PEG/ZIF-67 contained similar amounts of adsorbed polymer (Figure S2B). Even after controlling for the amount of adsorbed polymer—which includes polymer chains on the external surface and inside the pores—P4VP-b-PEG dispersions retained over 10× the O_2 carrying capacity of PEG dispersions (Figure S2C), which is consistent with the two polymers exhibiting different intrusion behaviors. This also suggests that any polymer micelle formation that may occur in solution does not contribute to differences in intrusion behavior.

Given that earlier studies have shown that aromatic molecules such as benzene, toluene, and xylene can diffuse through the pore apertures of ZIF-8 and ZIF-67,[44,45] it is likely that the large persistence length—and thus high backbone rigidity—of the aromatic polymer blocks is the primary factor that restricts their diffusion into the ZIF pores rather than the cross-sectional area of the PS or P4VP monomers. Moreover, since we did not observe any differences in the O_2 carrying capacity of ZIF particles modified with PS-b-PEG or P4VP-b-PEG, the hindered intrusion of copolymer chains can be

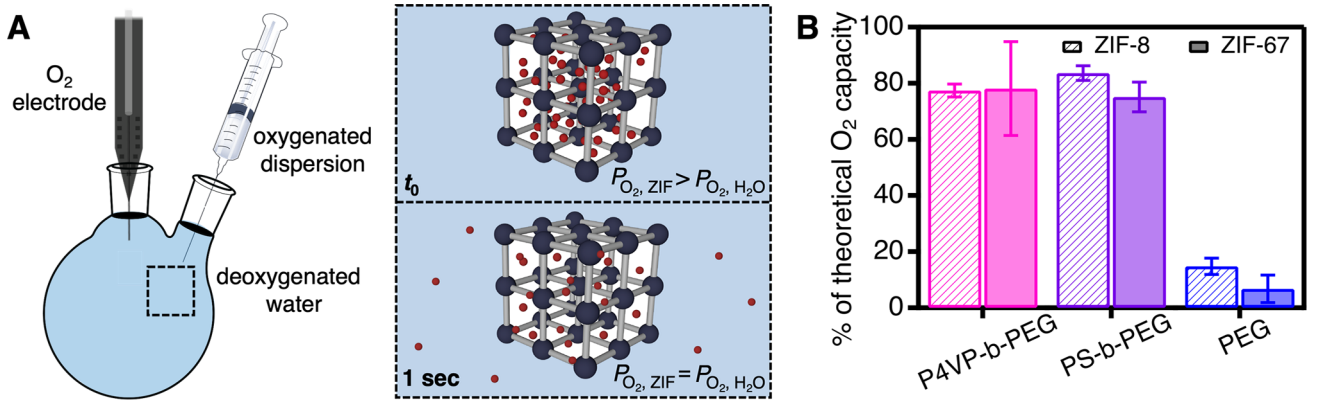

Figure 3. (A) Schematic illustration of the electrode-based setup used to quantify the O_2 carrying capacities of aqueous ZIF dispersions. (B) Measured O_2 carrying capacities—expressed as percentages of the theoretical expected value—for polymer/ZIF dispersions in water.

https://doi.org/10.1021/jacs.3c06627
J. Am. Chem. Soc. 2023, 145, 19982−19988

attributed primarily to chain rigidity rather than differences in the strength of polymer binding to the external ZIF surface.

Stability of Polymer-Functionalized ZIF Particles. Even though PS-b-PEG and P4VP-b-PEG both formed aqueous dispersions with the same microporosity, the block copolymers led to marked differences in the hydrolytic stability of the ZIF particles. Since ZIF-67 is substantially more prone to hydrolysis than ZIF-8 due to the greater lability of Co−imidazolate bonds compared to Zn−imidazolate, we focused our stability studies on ZIF-67 particles. Under dilute conditions (0.4 mg ZIF-67 per mL water), unfunctionalized ZIF-67 particles (average diameter = 910 nm ± 150 nm) degrade completely into a mixture of amorphous and crystalline cobalt hydroxide nanoparticles within 100 min (Figures 4A−D, S3). Notably, PEG and PS-b-PEG (at a 1:1

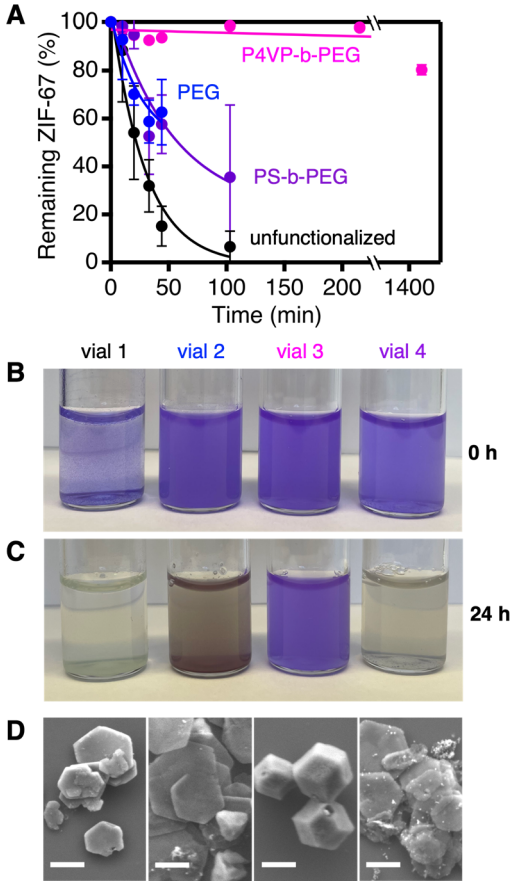

Figure 4. (A) Percentage of ZIF-67 particles remaining over time for dispersions of 0.4 mg ZIF-67 per mL water. (B) Images of ZIF-67 dispersions immediately after redispersing in water and (C) after 24 h. (D) Representative SEM images of dried ZIF-67 dispersions after 24 h in water (scale bars = 500 nm). In B−D, vial 1 contains unfunctionalized ZIF-67 particles, while vials 2, 3, and 4 contain ZIF-67 particles functionalized with PEG, P4VP-b-PEG, and PS-b-PEG, respectively, at a 1:1 polymer-to-ZIF mass ratio.

polymer-to-ZIF mass ratio) reduce the decomposition rate by over threefold, suggesting that the adsorbed polymers affect the accessibility of water molecules to the external ZIF surface. However, particles still start to aggregate after 50 min (Figure S4), and by 24 h the ZIF-67 particles fully convert into cobalt hydroxide byproducts. In contrast, ZIF-67 particles functionalized with P4VP-b-PEG retain complete dispersibility and over 80% of their gas carrying capacity even after 24 h. We attribute this enhanced hydrolytic stability to strong interactions between the pyridine groups of P4VP and coordinatively unsaturated Co sites on the external ZIF-67 surface,[32] which likely inhibit coordination of water molecules and slow down framework degradation.

At higher concentrations (30 mg ZIF per mL water) where the driving force for hydrolysis is reduced, both PS-b-PEG and P4VP-b-PEG stabilize ZIF-67 to a similar extent. After 10 days in water, ZIF-67 particles coated with either diblock copolymer retain over 80% of their O_2 carrying capacity, compared to less than 20% retention for unfunctionalized ZIF-67 over the same time (Figure S5). These results illustrate how noncovalent functionalization with polymers can dramatically enhance the hydrolytic stability of ZIFs in concentrated dispersions. At low concentrations, however, stronger interactions between the polymer and the ZIF surface are critical to promoting stability.

Mechanistic Insights into Polymer Infiltration. To provide additional insight into the interactions of amphiphilic polymers with ZIF particles, we evaluated the O_2 carrying capacity of aqueous dispersions as a function of polymer concentration at a fixed ZIF concentration. Since PS-b-PEG has poor water solubility above a ∼3:1 polymer:ZIF mass ratio, we evaluated the concentration dependence for PEG and P4VP-b-PEG. For P4VP-b-PEG, the O_2 carrying capacities of ZIF dispersions decrease with increasing polymer concentration to as low as 21% ± 4.3% for a 10:1 polymer:ZIF mass ratio, which shows that higher polymer concentrations drive additional intrusion into the ZIF nanocrystals (Figure 5A). Polymer intrusion is further confirmed through in situ wide-angle X-ray scattering (WAXS) experiments that show increased electron density in the framework pores at higher P4VP-b-PEG concentrations (Figure 5B). Specifically, the intensity of the 110 diffraction peak decreases substantially as the P4VP-b-PEG:ZIF ratio is increased from 1:1 to 4:1, which we attribute to an increased density of randomly oriented polymer chains intruding into the ZIF framework (Figure S6).[43] This is in contrast to PEG, for which the intensity of the 110 diffraction peak is already significantly reduced at a 1:1 PEG:ZIF ratio and remains constant with increasing PEG concentration (Figure 5C). The diffraction data is thus consistent with PEG fully infiltrating the ZIF pores even at low polymer concentrations.

The increased infiltration of P4VP-b-PEG at higher concentrations is likely to occur by one of two mechanisms: (1) the PEG segments of the adsorbed copolymers could exclusively intrude deeper into the ZIF core while the aromatic segments remain preferentially segregated to the external ZIF surface, or (2) both blocks of the polymer could intrude into the ZIF pores and distribute evenly throughout the framework. To determine which possibility is more likely, we measured the O_2 carrying capacity at a fixed polymer-to-ZIF ratio and fixed ZIF concentration (3 wt %) as a function of ZIF-8 particle size. Specifically, we used a 2:1 P4VP-b-PEG:ZIF-8 mass ratio—which ensured that enough adsorbed polymer was present to promote high colloidal stability—for four different average ZIF-8 particle diameters: 45 nm ± 6 nm, 235 nm ± 41 nm, 440 nm ± 58 nm, and 880 nm ± 74 nm. At this polymer loading, larger ZIF-8 particles retained a much higher O_2 carrying capacity than smaller particles. For instance, the smallest nanocrystals retained just 13% of their O_2 carrying capacity, while the largest nanocrystals retained 74% (Figure 6A). Since a greater fraction of the total volume of a particle is located closer to the external surface for larger particles (Figure

https://doi.org/10.1021/jacs.3c06627
J. Am. Chem. Soc. 2023, 145, 19982−19988

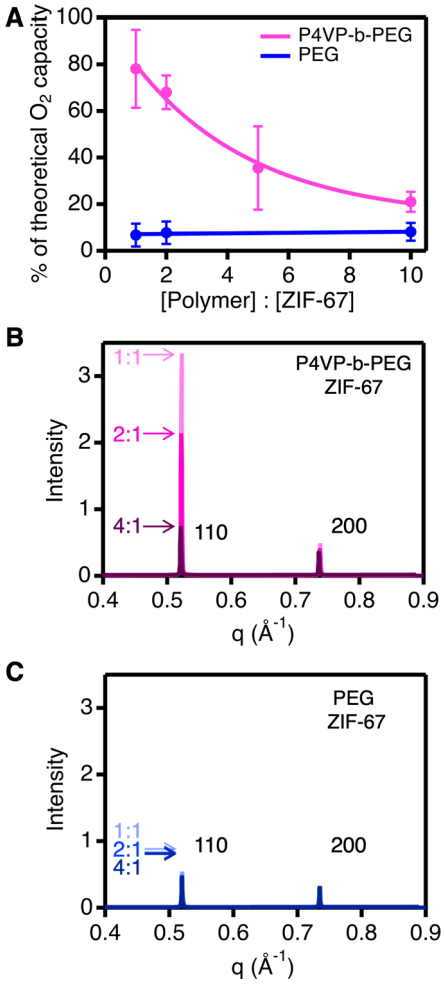

Figure 5. (A) Measured O_2 carrying capacities—expressed as percentages of the theoretical expected value—for polymer/ZIF-67 dispersions in water at different polymer loadings. (B) WAXS patterns of P4VP-b-PEG/ZIF-67 in water at different polymer loadings. (C) WAXS patterns of PEG/ZIF-67 in water at different polymer loadings. All data in this figure was acquired using ZIF-67 particles with an average diameter of 910 nm ± 150 nm.

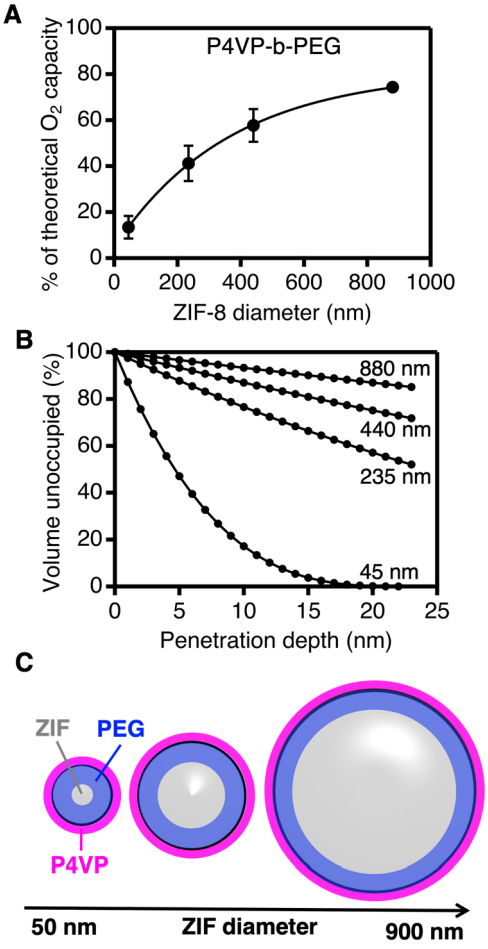

Figure 6. (A) O_2 carrying capacities—expressed as percentages of the theoretical expected value—for polymer/ZIF-8 dispersions in water with different average ZIF-8 particle sizes. (B) Percent of unoccupied volume for idealized ZIF spheres as a function of sphere diameter and polymer penetration depth. (C) Schematic illustration of how similar penetration depths of a diblock copolymer could result in large changes to the occupied pore volume of differently sized particles.

6B), the strong dependence of O_2 carrying capacity—and, consequently, permanent microporosity—on particle size is consistent with the aromatic segment limiting the distance over which entire polymer chains can infiltrate into the particle.

By treating the ZIF particles as spheres, we estimate that $P4VP_{3.5kDa}$-b-PEG_{10kDa} chains infiltrate between 30−40 nm into ZIF particles at a 2:1 polymer:ZIF ratio (Table S2). We note that this model is limited because we assume a single diameter for the particle size rather than a distribution of sizes. However, the estimated infiltration distance is much smaller than the length of a fully extended 10 kDa PEG block, which could extend up to ∼90 nm. Thus, the loss of O_2 capacity could be accounted for by PEG segments stretching into the ZIF pores even if the aromatic segments remain pinned near the external surface (Figure 6C). Moreover, WAXS patterns for different ZIF-8 particle sizes—at a fixed 2:1 P4VP-b-PEG:ZIF-8 mass ratio—are consistent with greater electron density—and, consequently, greater polymer pore filling—for smaller particles (Figure S7). As the polymer concentration is increased, more PEG chain segments would be forced deeper inside the ZIF pores, while the rigid aromatic segments would remain preferentially localized near the external surface of the particles. Though additional studies are in progress to confirm this proposed mechanism, the incorporation of rigid blocks into PEG-based polymers provides a promising strategy to inhibit polymer infiltration into hydrophobic metal−organic frameworks and to preserve a high gas carrying capacity in water.

CONCLUSIONS

The foregoing results illustrate how the interface between polymers and hydrophobic metal−organic frameworks can be engineered to promote dispersibility and stability in water while retaining gas-accessible permanent microporosity. Amphiphilic PEG-based polymers readily adsorb to the external surface of ZIF-8 and ZIF-67, allowing stable aqueous dispersions to be formed at ZIF concentrations as high as 8 vol %. Although flexible, narrow polymers like PEG readily infiltrate into the internal ZIF pores, block copolymers with rigid, bulky segments hinder polymer infiltration. Because the increased persistence length of the copolymers preferentially pins rigid blocks near the external ZIF surface, it is possible to retain large fractions (>75%) of the gas-accessible pore

https://doi.org/10.1021/jacs.3c06627
J. Am. Chem. Soc. 2023, 145, 19982−19988

volume—and, therefore, the gas carrying capacity—of hydrophobic ZIF nanocrystals in water. Further, polymer segments capable of engaging in strong interactions with the external ZIF surface dramatically enhance hydrolytic stability at low ZIF concentrations. Beyond providing new opportunities for designing aqueous porous liquids, our mechanistic insights into the infiltration behavior of polymers should be relevant to the use of polymer-functionalized metal−organic frameworks for mixed-matrix membranes,[23,24,46] polymerization templates,[47,48] and drug delivery.[12,49]

■ ASSOCIATED CONTENT

Supporting Information

The Supporting Information is available free of charge at https://pubs.acs.org/doi/10.1021/jacs.3c06627.

The PDF contains detailed experimental procedures, characterization, and additional supporting data (Supporting Tables S1−S2 and Supporting Figures S1−S7) (PDF).

■ AUTHOR INFORMATION

Corresponding Author

Jarad A. Mason − *Department of Chemistry and Chemical Biology, Harvard University, Cambridge, Massachusetts 02138, United States;* orcid.org/0000-0003-0328-7775; Email: mason@chemistry.harvard.edu

Authors

Christopher DelRe − *Department of Chemistry and Chemical Biology, Harvard University, Cambridge, Massachusetts 02138, United States*

Hyukhun Hong − *Department of Chemistry and Chemical Biology, Harvard University, Cambridge, Massachusetts 02138, United States*

Malia B. Wenny − *Department of Chemistry and Chemical Biology, Harvard University, Cambridge, Massachusetts 02138, United States*

Daniel P. Erdosy − *Department of Chemistry and Chemical Biology, Harvard University, Cambridge, Massachusetts 02138, United States;* orcid.org/0000-0002-0360-469X

Joy Cho − *Department of Chemistry and Chemical Biology, Harvard University, Cambridge, Massachusetts 02138, United States*

Byeongdu Lee − *X-ray Science Division, Argonne National Laboratory, Lemont, Illinois 60439, United States;* orcid.org/0000-0003-2514-8805

Complete contact information is available at: https://pubs.acs.org/10.1021/jacs.3c06627

Notes

The authors declare the following competing financial interest(s): C.D., M.B.W., D.P.E., J.C., and J.A.M. are inventors on a patent application related to microporous water held and submitted by Harvard University. The other authors declare no competing interests.

■ ACKNOWLEDGMENTS

This work was supported in part by a Multidisciplinary University Research Initiative, sponsored by the US Department of the Navy, Office of Naval Research, under grant no. N00014-20-1-2418 and by the US Department of the Navy, Office of Naval Research, under grant no. N00014-22-1-2739. This work was performed in part at the Harvard University Center for Nanoscale Systems (CNS); a member of the National Nanotechnology Coordinated Infrastructure Network (NNCI), which is supported by the National Science Foundation under NSF award no. ECCS 2025158. This research used resources of the Advanced Photon Source, a U.S. Department of Energy (DOE) Office of Science user facility operated for the DOE Office of Science by Argonne National Laboratory under Contract No. DE-AC02-06CH11357. J.A.M. acknowledges support from the Arnold and Mabel Beckman Foundation through a Beckman Young Investigator Grant. D.P.E. acknowledges support from a DoD National Defense Science and Engineering (NDSEG) fellowship.

■ ABBREVIATIONS

PEG	poly(ethylene glycol)
P4VP-b-PEG	poly(4-vinyl pyridine)-block-poly(ethylene glycol)
PS-b-PEG	poly(styrene)-block-poly(ethylene glycol)
ZIF-8	zeolitic imidazolate framework-8
ZIF-67	zeolitic imidazolate framework-67

■ REFERENCES

(1) Fox, E. B.; Colon-Mercado, H. R. Mass Transport Limitations in Proton Exchange Membrane Fuel Cells and Electrolyzers. *Mass Transfer - Advanced Aspects*; IntechOpen 2011, 305 −318.

(2) Peng, Y. F.; Kheir, J. N.; Polizzotti, B. D. Injectable Oxygen: Interfacing Materials Chemistry with Resuscitative Science. *Chem.-Eur. J.* **2018**, *24*, 18820−18829.

(3) Garcia-Ochoa, F.; Gomez, E. Bioreactor scale-up and oxygen transfer rate in microbial processes: An overview. *Biotechnol. Adv.* **2009**, *27*, 153−176.

(4) Guibert, E. E.; Petrenko, A. Y.; Balaban, C. L.; Somov, A. Y.; Rodriguez, J. V.; Fuller, B. J. Organ Preservation: Current Concepts and New Strategies for the Next Decade. *Transfus. Med. Hemother.* **2011**, *38*, 125−142.

(5) Thorarinsdottir, A. E.; Erdosy, D. P.; Costentin, C.; Mason, J. A.; Nocera, D. G. Enhanced activity for the oxygen reduction reaction in microporous water. *Nat. Catal.* **2023**, *6*, 425−434.

(6) Furukawa, H.; Cordova, K. E.; O'Keeffe, M.; Yaghi, O. M. The Chemistry and Applications of Metal-Organic Frameworks. *Science* **2013**, *341*, No. 1230444.

(7) Li, J. Y.; Corma, A.; Yu, J. H. Synthesis of new zeolite structures. *Chem. Soc. Rev.* **2015**, *44*, 7112−7127.

(8) Erdosy, D. P.; Wenny, M. B.; Cho, J.; DelRe, C.; Walter, M. V.; Jimenez-Angeles, F.; Qiao, B.; Sanchez, R.; Peng, Y.; Polizzotti, B. D.; de la Cruz, M. O.; Mason, J. A. Microporous water with high gas solubilities. *Nature* **2022**, *608*, 712−718.

(9) McGuire, C. V.; Forgan, R. S. The surface chemistry of metal-organic frameworks. *Chem. Commun.* **2015**, *51*, 5199−5217.

(10) Zimpel, A.; Preiss, T.; Röder, R.; Engelke, H.; Ingrisch, M.; Peller, M.; Rädler, J. O.; Wagner, E.; Bein, T.; Lächelt, U.; Wuttke, S. Imparting Functionality to MOF Nanoparticles by External Surface Selective Covalent Attachment of Polymers. *Chem. Mater.* **2016**, *28*, 3318−3326.

(11) Figueroa-Quintero, L.; Villalgordo-Hernandez, D.; Delgado-Marin, J. J.; Narciso, J.; Velisoju, V. K.; Castano, P.; Gascon, J.; Ramos-Fernandez, E. V. Post-Synthetic Surface Modification of Metal-Organic Frameworks and Their Potential Applications. *Small Methods* **2023**, *7*, No. e2201413.

(12) Della Rocca, J.; Liu, D. M.; Lin, W. B. Nanoscale Metal-Organic Frameworks for Biomedical Imaging and Drug Delivery. *Acc. Chem. Res.* **2011**, *44*, 957−968.

(13) Kalaj, M.; Bentz, K. C.; Ayala, S.; Palomba, J. M.; Barcus, K. S.; Katayama, Y.; Cohen, S. M. MOF-Polymer Hybrid Materials: From

Simple Composites to Tailored Architectures. *Chem. Rev.* **2020**, *120*, 8267−8302.
(14) Degennes, P. G. Scaling Theory of Polymer Adsorption. *J. Phys.* **1976**, *37*, 1445−1452.
(15) Cosgrove, T.; Griffiths, P. C.; Lloyd, P. M. Polymer Adsorption − the Effect of the Relative Sizes of Polymer and Particle. *Langmuir* **1995**, *11*, 1457−1463.
(16) Penna, M. J.; Mijajlovic, M.; Biggs, M. J. Molecular-Level Understanding of Protein Adsorption at the Interface between Water and a Strongly Interacting Uncharged Solid Surface. *J. Am. Chem. Soc.* **2014**, *136*, 5323−5331.
(17) Balazs, A. C.; Emrick, T.; Russell, T. P. Nanoparticle polymer composites: Where two small worlds meet. *Science* **2006**, *314*, 1107−1110.
(18) Moore, T. L.; Rodriguez-Lorenzo, L.; Hirsch, V.; Balog, S.; Urban, D.; Jud, C.; Rothen-Rutishauser, B.; Lattuada, M.; Petri-Fink, A. Nanoparticle colloidal stability in cell culture media and impact on cellular interactions. *Chem. Soc. Rev.* **2015**, *44*, 6287−6305.
(19) Harris, J. M.; Chess, R. B. Effect of pegylation on pharmaceuticals. *Nat. Rev. Drug Discov.* **2003**, *2*, 214−221.
(20) Zhang, Z. J.; Nguyen, H. T. H.; Miller, S. A.; Ploskonka, A. M.; DeCoste, J. B.; Cohen, S. M. Polymer-Metal-Organic Frameworks (polyMOFs) as Water Tolerant Materials for Selective Carbon Dioxide Separations. *J. Am. Chem. Soc.* **2016**, *138*, 920−925.
(21) Shih, Y. H.; Kuo, Y. C.; Lirio, S.; Wang, K. Y.; Lin, C. H.; Huang, H. Y. A Simple Approach to Enhance the Water Stability of a Metal-Organic Framework. *Chem.-Eur. J.* **2017**, *23*, 42−46.
(22) Yang, S. L.; Karve, V. V.; Justin, A.; Kochetygov, I.; Espin, J.; Asgari, M.; Trukhina, O.; Sun, D. T.; Peng, L.; Queen, W. L. Enhancing MOF performance through the introduction of polymer guests. *Coord. Chem. Rev.* **2021**, *427*, No. 213525.
(23) Dong, G. X.; Li, H. Y.; Chen, V. K. Challenges and opportunities for mixed-matrix membranes for gas separation. *J. Mater. Chem. A* **2013**, *1*, 4610−4630.
(24) Galizia, M.; Chi, W. S.; Smith, Z. P.; Merkel, T. C.; Baker, R. W.; Freeman, B. D. 50th Anniversary Perspective: Polymers and Mixed Matrix Membranes for Gas and Vapor Separation: A Review and Prospective Opportunities. *Macromolecules* **2017**, *50*, 7809−7843.
(25) Zimpel, A.; Al Danaf, N.; Steinborn, B.; Kuhn, J.; Hohn, M.; Bauer, T.; Hirschle, P.; Schrimpf, W.; Engelke, H.; Wagner, E.; Barz, M.; Lamb, D. C.; Lachelt, U.; Wuttke, S. Coordinative Binding of Polymers to Metal-Organic Framework Nanoparticles for Control of Interactions at the Biointerface. *ACS Nano* **2019**, *13*, 3884−3895.
(26) Semino, R.; Moreton, J. C.; Ramsahye, N. A.; Cohen, S. M.; Maurin, G. Understanding the origins of metal-organic framework/polymer compatibility. *Chem. Sci.* **2018**, *9*, 315−324.
(27) Karakoti, A. S.; Das, S.; Thevuthasan, S.; Seal, S. PEGylated Inorganic Nanoparticles. *Angew. Chem., Int. Ed.* **2011**, *50*, 1980−1994.
(28) Lee, H.; Venable, R. M.; MacKerell, A. D., Jr.; Pastor, R. W. Molecular dynamics studies of polyethylene oxide and polyethylene glycol: Hydrodynamic radius and shape anisotropy. *Biophys. J.* **2008**, *95*, 1590−1599.
(29) Duan, P.; Moreton, J. C.; Tavares, S. R.; Semino, R.; Maurin, G.; Cohen, S. M.; Schmidt-Rohr, K. Polymer Infiltration into Metal-Organic Frameworks in Mixed-Matrix Membranes Detected in Situ by NMR. *J. Am. Chem. Soc.* **2019**, *141*, 7589−7595.
(30) Oe, N.; Hosono, N.; Uemura, T. Revisiting molecular adsorption: unconventional uptake of polymer chains from solution into sub-nanoporous media. *Chem. Sci.* **2021**, *12*, 12576.
(31) Kwiatkowski, A. L.; Sharma, H.; Molchanov, V. S.; Orekhov, A. S.; Vasiliev, A. L.; Dormidontova, E. E.; Philippova, O. E. Wormlike Surfactant Micelles with Embedded Polymer Chains. *Macromolecules* **2017**, *50*, 7299−7308.
(32) Knebel, A.; Bavykina, A.; Datta, S. J.; Sundermann, L.; Garzon-Tovar, L.; Lebedev, Y.; Durini, S.; Ahmad, R.; Kozlov, S. M.; Shterk, G.; Karunakaran, M.; Carja, I. D.; Simic, D.; Weilert, I.; Kluppel, M.; Giese, U.; Cavallo, L.; Rueping, M.; Eddaoudi, M.; Caro, J.; Gascon, J. Solution processable metal-organic frameworks for mixed matrix membranes using porous liquids. *Nat. Mater.* **2020**, *19*, 1346−1353.
(33) Burtch, N. C.; Jasuja, H.; Walton, K. S. Water Stability and Adsorption in Metal-Organic Frameworks. *Chem. Rev.* **2014**, *114*, 10575−10612.
(34) Chen, S.; Guo, C.; Hu, G. H.; Wang, J.; Ma, J. H.; Liang, X. F.; Zheng, L.; Liu, H. Z. Effect of hydrophobicity inside PEO-PPO-PEO block copolymer micelles on the stabilization of gold nanoparticles: Experiments. *Langmuir* **2006**, *22*, 9704−9711.
(35) Hamed, E.; Xu, T.; Keten, S. Poly(ethylene glycol) Conjugation Stabilizes the Secondary Structure of alpha-Helices by Reducing Peptide Solvent Accessible Surface Area. *Biomacromolecules* **2013**, *14*, 4053−4060.
(36) Park, K. S.; Ni, Z.; Cote, A. P.; Choi, J. Y.; Huang, R. D.; Uribe-Romo, F. J.; Chae, H. K.; O'Keeffe, M.; Yaghi, O. M. Exceptional chemical and thermal stability of zeolitic imidazolate frameworks. *Proc. Natl. Acad. Sci. U. S. A.* **2006**, *103*, 10186−10191.
(37) Banerjee, R.; Phan, A.; Wang, B.; Knobler, C.; Furukawa, H.; O'Keeffe, M.; Yaghi, O. M. High-throughput synthesis of zeolitic imidazolate frameworks and application to CO_2 capture. *Science* **2008**, *319*, 939−943.
(38) Ortiz, G.; Nouali, H.; Marichal, C.; Chaplais, G.; Patarin, J. Energetic performances of the metal-organic framework ZIF-8 obtained using high pressure water intrusion-extrusion experiments. *Phys. Chem. Chem. Phys.* **2013**, *15*, 4888−4891.
(39) Khay, I.; Chaplais, G.; Nouali, H.; Marichal, C.; Patarin, J. Water intrusion-extrusion experiments in ZIF-8: impacts of the shape and particle size on the energetic performances. *RSC Adv.* **2015**, *5*, 31514−31518.
(40) Cravillon, J.; Münzer, S.; Lohmeier, S. J.; Feldhoff, A.; Huber, K.; Wiebcke, M. Rapid Room-Temperature Synthesis and Characterization of Nanocrystals of a Prototypical Zeolitic Imidazolate Framework. *Chem. Mater.* **2009**, *21*, 1410−1412.
(41) Taheri, M.; Enge, T. G.; Tsuzuki, T. Water stability of cobalt doped ZIF-8: a quantitative study using optical analyses. *Mater. Today Chem.* **2020**, *16*, No. 100231.
(42) Schoenecker, P. M.; Carson, C. G.; Jasuja, H.; Flemming, C. J. J.; Walton, K. S. Effect of Water Adsorption on Retention of Structure and Surface Area of Metal-Organic Frameworks. *Ind. Eng. Chem. Res.* **2012**, *51*, 6513−6519.
(43) Choi, M.; Kleitz, F.; Liu, D. N.; Lee, H. Y.; Ahn, W. S.; Ryoo, R. Controlled polymerization in mesoporous silica toward the design of organic-inorganic composite nanoporous materials. *J. Am. Chem. Soc.* **2005**, *127*, 1924−1932.
(44) Ueda, T.; Yamatani, T.; Okumura, M. Dynamic Gate Opening of ZIF-8 for Bulky Molecule Adsorption as Studied by Vapor Adsorption Measurements and Computational Approach. *J. Phys. Chem. C* **2019**, *123*, 27542−27553.
(45) Polyukhov, D. M.; Poryvaev, A. S.; Sukhikh, A. S.; Gromilov, S. A.; Fedin, M. V. Fine-Tuning Window Apertures in ZIF-8/67 Frameworks by Metal Ions and Temperature for High-Efficiency Molecular Sieving of Xylenes. *ACS Appl. Mater. Interfaces* **2021**, *13*, 40830−40836.
(46) Wang, W.; Chai, M.; Zulkifli, M. Y. B.; Xu, K.; Chen, Y.; Wang, L.; Chen, V.; Hou, J. Metal−Organic Framework Composites from Mechanochemical Processes. *Mol. Syst. Des. Eng.* **2023**, *8*, 560−579.
(47) Schmidt, B. V. K. J. Metal-Organic Frameworks in Polymer Science: Polymerization Catalysis, Polymerization Environment, and Hybrid Materials. *Macromol. Rapid Commun.* **2020**, *41*, No. 1900333.
(48) Kitao, T.; Zhang, X.; Uemura, T. Nanoconfined synthesis of conjugated ladder polymers. *Polym. Chem.* **2022**, *13*, 5003−5018.
(49) Lawson, H. D.; Walton, S. P.; Chan, C. Metal-Organic Frameworks for Drug Delivery: A Design Perspective. *ACS Appl. Mater. Interfaces* **2021**, *13*, 7004−7020.

https://doi.org/10.1021/jacs.3c06627
J. Am. Chem. Soc. 2023, 145, 19982−19988